

Mixing antiferromagnets to tune NiFe-[IrMn/FeMn] interfacial spin-glasses, grains thermal stability, and related exchange bias properties

K. Akmalidinov, C. Ducruet, C. Portemont, I. Joumard, I. L. Prejbeanu, B. Dieny, Vincent Baltz

► **To cite this version:**

K. Akmalidinov, C. Ducruet, C. Portemont, I. Joumard, I. L. Prejbeanu, et al.. Mixing antiferromagnets to tune NiFe-[IrMn/FeMn] interfacial spin-glasses, grains thermal stability, and related exchange bias properties. *Journal of Applied Physics*, American Institute of Physics, 2014, 115, pp.17B718. 10.1063/1.4864144 . hal-01683648

HAL Id: hal-01683648

<https://hal.archives-ouvertes.fr/hal-01683648>

Submitted on 19 May 2019

HAL is a multi-disciplinary open access archive for the deposit and dissemination of scientific research documents, whether they are published or not. The documents may come from teaching and research institutions in France or abroad, or from public or private research centers.

L'archive ouverte pluridisciplinaire **HAL**, est destinée au dépôt et à la diffusion de documents scientifiques de niveau recherche, publiés ou non, émanant des établissements d'enseignement et de recherche français ou étrangers, des laboratoires publics ou privés.



Mixing antiferromagnets to tune NiFe-[IrMn/FeMn] interfacial spin-glasses, grains thermal stability, and related exchange bias properties

K. Akmalinov,^{1,2} C. Ducret,² C. Portemont,² I. Joumard,¹ I. L. Prejbeanu,¹ B. Dieny,¹ and V. Baltz^{1,a)}

¹SPINTEC, UMR 8191 CNRS/INAC-CEA/UJF-Grenoble 1/Grenoble-INP, F-38054 Cedex, France

²CROCUS Technology, F-38025 Grenoble, France

(Presented 6 November 2013; received 19 September 2013; accepted 4 November 2013; published online 6 February 2014)

Spintronics devices and in particular thermally assisted magnetic random access memories require a wide range of ferromagnetic/antiferromagnetic (F/AF) exchange bias (EB) properties and subsequently of AF materials to fulfil diverse functionality requirements for the reference and storage. For the reference layer, large EB energies and high blocking temperature (T_B) are required. In contrast, for the storage layer, mostly moderate T_B are needed. One of the present issues is to find a storage layer with properties intermediate between those of IrMn and FeMn and in particular: (i) with a T_B larger than FeMn for better stability at rest-T but lower than IrMn to reduce power consumption at write-T and (ii) with improved magnetic interfacial quality, i.e., with reduced interfacial glassy character for lower properties dispersions. To address this issue, the EB properties of F/AF based stacks were studied for various mixed [IrMn/FeMn] AFs. In addition to EB loop shifts, the F/AF magnetic interfacial qualities and the AF grains thermal stability are probed via measurements of the low- and high-temperature contributions to the T_B distributions, respectively. A tuning of the above three parameters is observed when evolving from IrMn to FeMn via [IrMn/FeMn] repetitions. © 2014 AIP Publishing LLC. [<http://dx.doi.org/10.1063/1.4864144>]

Spintronics thermally assisted magnetic random access memories (TA-MRAM) applications¹ use two ferromagnetic/antiferromagnetic (F/AF) exchange bias (EB) bilayers:² one for reference and one for storage. The blocking temperature (T_B) is the temperature (T) above which the F is no longer pinned by the AF. It depends on various parameters among which the F/AF interfacial coupling, the AF bulk properties and time.² In particular, T_B increases with the F magnetization sweep-rate.^{3,4} At rest-T, both the reference and storage layers magnetization must withstand thermal activation, i.e., T_B must be much larger than the rest-T. During writing, the TA-MRAM cell is simultaneously heated for a few nanoseconds at a T of about 200 °C thanks to a current flowing through the tunnel barrier and subjected to a magnetic field pulse of tens of Oersteds. The reference layer with a high T_B (e.g., pinned to PtMn²) remains unaffected by this. In contrast, the storage layer with a moderate T_B (e.g., pinned to IrMn or FeMn²) unpins at the write-T so that its magnetization switches in the applied field direction.¹ Engineering the storage layer thus requires compromises since its critical-T needs to be adjusted above the rest-T but below the write-T. TA-MRAM are mostly based on PtMn for the reference layer and IrMn or FeMn for the storage one.^{1,5} One of the present industrial issues with regards to TA-MRAM is to find a storage layer with intermediate properties between those of IrMn and FeMn and in particular with a critical-T larger than FeMn for better stability at rest-T but lower than IrMn to reduce power consumption at write-T. Another issue concerns the magnetic interfacial quality, i.e., the amount of

interfacial spin-glasses that need to be as small as possible since it is believed to mainly contribute to cell to cell dispersions after patterning the sheet film.¹⁷ Additives like Cr enhance AFs corrosion and stress resistance. To some extent, they also tune the AF Néel-T, the F/AF T_B , and the loop shift amplitude (H_E).⁶⁻⁸ To this adds AF laminations⁹ and stoichiometry adjustments in the range where the compounds remain AF.¹⁰⁻¹³ Varying the layers thicknesses is another way to enlarge the range of EB properties since, for example, H_E is inversely proportional to the F thickness and T_B depends on the AF thickness.² Yet, most of these adjustments either do not influence the F/AF interface or neglect their impact on the amount of interfacial spin-glass like phases.¹⁴⁻¹⁹ For example, although varying the AF (e.g., IrMn) thickness reduces T_B , it makes no difference on the amount of interfacial spin-glasses. Via the combination of a specific procedure commonly carried out for measurements of T_B distributions (DT_B) above room-T²⁰ and the alternative use of a sufficiently low reference-T¹⁷ (usually 4 K), we recently quantified the magnetic interfacial quality of F/AF bilayers (i.e., the interfacial glassy character).¹⁷⁻¹⁹ The method is fairly easy to implement in laboratories and provides data usually obtained via large scale facilities experiments. For example, x-ray magnetic circular dichroism results obtained from synchrotron radiation experiments give the amount of frozen AF spins, at room-T usually,²¹ when our laboratory method provides the complement, i.e., the amount of unfrozen spins at and above room-T.¹⁷⁻¹⁹

The present study focuses on finding an appropriate AF material for EB of the storage layer in TA-MRAM with intermediate properties between those of IrMn and FeMn. It mixes

^{a)}Electronic mail: vincent.baltz@cea.fr.

usual IrMn and FeMn in the form of [IrMn/FeMn] repetitions in an attempt to widen the coverage of available AFs and F/AF properties; interface quality included^{14–19} for the storage layer. Therefore, in addition to EB loop shifts, the F/AF magnetic interfacial qualities^{14–19} and the AF grains thermal stability^{22–24} are studied via measurements of the low-¹⁷ and high-temperature²² contributions to DT_B , respectively.

For this work, buffer/CoFeB (1.2 nm)/Mg (1.4 nm, naturally oxidized)/F/AF/Ta (5 nm), with F = CoFeB (2 nm)/NiFe (1.5 nm) and AF = IrMn (10 nm), [IrMn (t nm)/FeMn (t nm)]_{xN}, [FeMn (t nm)/IrMn (t nm)]_{xN} and FeMn (10 nm), are deposited onto silicon substrates by sputtering.³ The IrMn and FeMn thicknesses t and the number of repetitions N take the following values so that the total thickness of the AF is constant at 10 nm: $(t:N) = (2.5:2)$ and $(1:5)$. After deposition, room-T EB is set by field cooling (FC) the samples in a furnace from 573 K for 90 min down to room-T. The magnetic field applied during cooling is positive in the sample plane and its amplitude of 10 kOe saturates the CoFeB (2 nm)/NiFe (1.5 nm) F layer. In addition, the T of 573 K is large enough so that, following this initial FC, all the AF entities with T_B larger than room-T are oriented toward the positive direction.¹⁷ Hysteresis loops are then measured at room-T. Subsequent initial positive FC is continued down to 4 K in a vibrating sample magnetometer (VSM). DT_B in the range of 4–473 K are then deduced from hysteresis loops measured at 4 K by VSM after a specific procedure which includes FC from incremental annealing temperatures (T_a). The typical evolution of hysteresis loops after various T_a is shown elsewhere.^{17,20}

Figure 1 shows the variations with T_a of the normalized loop shifts, $H_E/H_E(T_a = 4\text{ K})$ and the corresponding derivatives for our F/AF multilayers with various AFs. From the initial state where all the AF entities contributing to EB are oriented positively, the procedure consists in gradually reversing the AF entities by use of negative FC down to 4 K from incremental T_a . After each increment of T_a , a hysteresis loop is measured at 4 K. Its shift in field, H_E , integrates AF entities with T_B larger than T_a (unaffected by the FC at T_a and still initially oriented positively) minus AF entities with T_B lower than T_a (reoriented negatively). A gradual change in the amplitude and sign of H_E is observed in Fig. 1(a) since the higher the T_a , the more the reversed entities. In addition and by definition, the derivative $\delta H_E/\delta T_a$ vs T_a in Fig. 1(b) corresponds to DT_B .¹⁷ Thus: (i) an inflection point for H_E vs T_a denotes a peak in the distribution and (ii) the amplitude Δ around the inflection is the surface, S of the corresponding peak (see Fig. 1). In the following, Δ is the difference between H_E after $T_a = 4$ and 200 K (i.e., after the low-T inflection). The two contributions to DT_B can be observed in Fig. 1. The low-T contribution is known to originate from AF interfacial spin-glass-like phases.^{14–19} Given that, Δ [Fig. 1(a)] or S [Fig. 1(b)] measures the glassy character of the interface. In the following and to ease the interpretation, this glassy character is expressed in percentage: Δ^* equals Δ normalized to the total expected variations of H_E , i.e., 2 for normalized H_E . The second inflection point in the H_E vs T_a variations [Fig. 1(a)] corresponds to the high-T contribution to DT_B [Fig. 1(b)] and is related to the grains stability and

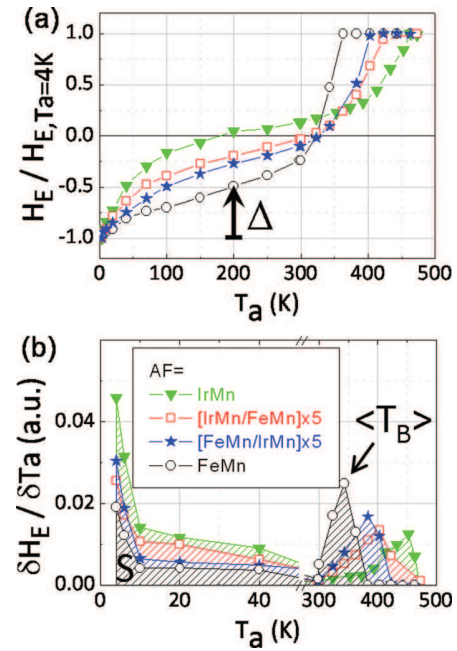


FIG. 1. (a) Typical variations with the annealing temperatures (T_a) of the normalized loop shift ($H_E/H_E(T_a = 4\text{ K})$) deduced from hysteresis loops measured at 4 K by VSM for CoFeB (2 nm)/NiFe (1.5 nm)/AF, subject to a procedure detailed within the text and involving various T_a . The AF layers are: IrMn (10 nm), [IrMn (1 nm)/FeMn (1 nm)]_{x5}, [FeMn (1 nm)/IrMn (1 nm)]_{x5} and FeMn (10 nm). (b) Variations with T_a of $\delta H_E/\delta T_a$ representing the blocking temperature distributions.

sizes dispersion.^{22–24} This contribution is centred on $\langle T_B \rangle$ [see Fig. 1(b)].

For the various AFs, Fig. 2(a) shows the amount of interfacial spin-glass, Δ^* deduced from Fig. 1(a). The F/AF magnetic interfacial quality varies from a glassy interface with IrMn ($\sim 52\%$) to a twice less glassy interface with FeMn ($\sim 25\%$) via an intermediate value with [IrMn(t)/FeMn(t)]_{xN} repetitions ($\sim 38\%$). The differences between IrMn (Ir₂₀Mn₈₀) and FeMn (Fe₅₀Mn₅₀) were already observed and ascribed to the larger proportion of Mn atoms for the IrMn.^{17,18} It was inferred that the larger the amount of Mn atoms, the more glassy the interface. In particular, Mn atoms diffuse at the interface and create spin-glass phases. Lowering this via the addition of diffusion barriers was recently evidenced.²⁵ The intermediate value obtained with [IrMn(t)/FeMn(t)]_{xN} repetitions is independent on the repetitions parameters $(t:N)$. This implies that alloys likely form rather than well separated layers and well defined interfaces within the repetition. This is surely related to layers intermixing and alloying occurring during both deposition and post-deposition FC from 573 K (Refs. 26–30). Although the science of layers interdiffusion at the atomic scale involves many complex aspects out of the scope of the present article, one of the major empirical conclusions here is that simply stacking (alloying) IrMn and FeMn offers a knob to tune the magnetic interface quality exactly between that of pure IrMn and FeMn.

Figure 2(b) shows the hysteresis loop shift amplitude, H_E measured at $T_m = 4$ and 300 K for the various AFs. For a given T_m , H_E is related to many parameters such as the

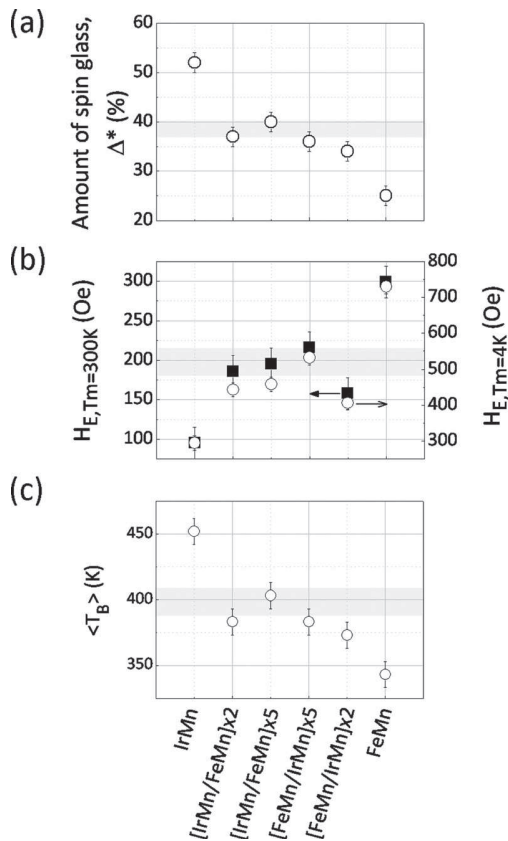


FIG. 2. For CoFeB (2 nm)/NiFe (1.5 nm)/AF, with AF = IrMn (10 nm), [IrMn (t nm)/FeMn (t nm)]_{xN}, [FeMn (t nm)/IrMn (t nm)]_{xN} and FeMn (10 nm), (t;N) = (2.5;2) and (1;5): (a) amount of spin-glass, $\Delta^* = \Delta/2$, see Fig. 1(a); (b) hysteresis loop shift, H_E measured at $T_m = 4$ and 300 K and (c) mean blocking temperature, of the high-T contribution, see Fig. 1(b). For every plot, the grey area is, within error bars, the mean value calculated from the IrMn and FeMn experimental data.

magnetic anisotropies of the F and AF (K_F , K_{AF}), the F-AF interfacial exchange stiffness (J_{F-AF}), the F and AF magnetic moments (m_F , m_{AF}), and the amount of AF entities that remain pinned when cycling the F.^{2,17} Although this latter parameter itself results as well from a complex compromise between J_{F-AF} , AF-AF exchange stiffness (J_{AF-AF}), grains volumes, amount of spin-glasses on top of each grain, etc., the DT_B plotted in Fig. 1(b) directly measures the relative amount of AF entities remaining pinned at $T = T_a$. Essentially, H_E measured at T_m is proportional to a complex function that depends on T_m and includes the above cited parameters: $g(T_m)$, times the integrand of the DT_B from the initial FC-T (here 573 K) to T_m .¹⁷ The increase of H_E between 4 and 300 K observed in Fig. 2(b) for all samples is ascribed both to the thermal variations of the intrinsic physical parameters and to the fact that more AF entities are frozen at 4 K than at 300 K [see Fig. 1(b)]. Figure 2(b) also shows that the [IrMn(t)/FeMn(t)]_{xN} alloys all have similar values intermediate between those of IrMn and FeMn: $H_{E,FeMn} > H_{E,[IrMn/FeMn]} > H_{E,IrMn}$. This is partly due to J_{F-AF} : FeMn coupled to NiFe shows larger J_{F-AF} than IrMn. Additionally, it

looks consistent that $J_{NiFe-[IrMn/FeMn]}$ stands between $J_{NiFe-FeMn}$ and $J_{NiFe-IrMn}$ since as measured and discussed above, the [IrMn(t)/FeMn(t)]_{xN} magnetic interface quality is intermediate between FeMn and IrMn. The differences between $H_{E,FeMn}$, $H_{E,[IrMn/FeMn]}$ and $H_{E,IrMn}$ are also in part related to the amount of stable AF entities which is larger for FeMn compared to [IrMn(t)/FeMn(t)]_{xN} and IrMn.

Figure 2(c) represents the mean T_B of the high-T contribution, extracted from Fig. 1(b). The [IrMn(t)/FeMn(t)]_{xN} repetitions all show similar values of $\langle T_B \rangle$ which confirms the likely formation of alloys rather than distinct layers separated by defined interfaces. Contrary to Fig. 1(a) where only the magnetic interfacial quality is probed, $\langle T_B \rangle$ is associated with the AF grains stability over F magnetization reversal, and is related to both the coupling of the AF to the F (J_{F-AF}) and the intrinsic thermal stability of the AF grains ($K_{AF} \cdot V_{AF}$).^{17,22–24} It seems that alloying IrMn and FeMn also results in AF grains stabilities intermediate between IrMn and FeMn.

To conclude, the F/AF storage layer building block of spintronics devices was studied. Alloying IrMn and FeMn offered an additional knob, easy to implement, to adjust at the same time the interfacial glassy character, H_E and AF grains stability to values intermediate between those of IrMn and FeMn. This responds to an industrial need and in particular provides an ideal material for a TA-MRAM storage layer with better stability than FeMn at rest-T but requiring less write power consumption than IrMn and with improved magnetic interfacial quality compared to IrMn.

¹I. L. Prejbeanu *et al.*, *J. Phys. D: Appl. Phys.* **46**, 074002 (2013).

²J. Nogués and I. K. Schuller, *J. Magn. Magn. Mater.* **192**, 203 (1999); A. E. Berkowitz and K. Takano, *ibid.* **200**, 552 (1999).

³L. Lombard *et al.*, *J. Appl. Phys.* **107**, 09D728 (2010).

⁴C. Papusoi *et al.*, *J. Appl. Phys.* **104**, 013915 (2008).

⁵J. P. Nozières *et al.*, *J. Appl. Phys.* **87**, 3920 (2000).

⁶M. J. Carey *et al.*, *Appl. Phys. Lett.* **81**, 5198 (2002).

⁷T. Ohtsu *et al.*, *IEEE Trans. Magn.* **43**, 2211 (2007).

⁸B. Dai *et al.*, *Appl. Phys. Lett.* **85**, 5281 (2004).

⁹G. W. Anderson and Y. M. Huai, *J. Appl. Phys.* **87**, 4924 (2000).

¹⁰S.-S. Lee *et al.*, *J. Appl. Phys.* **95**, 7525 (2004).

¹¹T. Yamaoka *et al.*, *J. Phys. Soc. Japan* **31**, 301 (1971).

¹²Y. Endoh and Y. Ishikawa, *J. Phys. Soc. Japan* **30**, 1614 (1971).

¹³P. F. Ladwig *et al.*, *J. Appl. Phys.* **94**, 979 (2003).

¹⁴K. Takano *et al.*, *Phys. Rev. Lett.* **79**, 1130 (1997).

¹⁵J. Ventura *et al.*, *J. Appl. Phys.* **101**, 113901 (2007).

¹⁶M. Ali *et al.*, *Nature Mater.* **6**, 70 (2007).

¹⁷V. Baltz *et al.*, *Phys. Rev. B* **81**, 052404 (2010).

¹⁸V. Baltz, *Appl. Phys. Lett.* **102**, 062410 (2013).

¹⁹V. Baltz *et al.*, *Appl. Phys. Lett.* **96**, 262505 (2010).

²⁰S. Soeya *et al.*, *J. Appl. Phys.* **76**, 5356 (1994).

²¹J. Wu *et al.*, *Phys. Rev. Lett.* **104**, 217204 (2010).

²²E. Fulcomer and S. H. Charap, *J. Appl. Phys.* **43**, 4190 (1972).

²³V. Baltz *et al.*, *Phys. Rev. B* **72**, 104419 (2005).

²⁴K. O'Grady *et al.*, *J. Magn. Magn. Mater.* **322**, 883 (2010).

²⁵K. Akmalidinov *et al.*, *Appl. Phys. Lett.* **103**, 042415 (2013).

²⁶R. M. Bozorth, *Ferromagnetism* (D. Van Nostrand Company Inc., 1951).

²⁷X. W. Zhou *et al.*, *Acta Mater.* **49**, 4005 (2001).

²⁸L. Lechevallier *et al.*, *J. Appl. Phys.* **112**, 043904 (2012).

²⁹F. Letellier *et al.*, *J. Phys. D: Appl. Phys.* **45**, 275001 (2012).

³⁰M.-A. Nicolet, *Thin Solid Films* **52**, 415 (1978).